Acc. Chem. Res. **2004,** *37,* 231−241

Do New Century Catalysts Unravel the Mechanism of Stereocontrol of Old Ziegler−Natta Catalysts?

PAOLO CORRADINI,† GAETANO GUERRA,‡ AND LUIGI CAVALLO*,‡

Dipartimento di Chimica, Università di Napoli, Via Cintia, I-80136 Napoli, Italy, Dipartimento di Chimica, Università di Salerno, Via Salvador Allende, I-84081 Baronissi (SA), Italy

Received June 4, 2003

ABSTRACT

Stereoselective polymerization of 1-alkenes was discovered 50 years ago. However, a detailed knowledge of the traditional and industrially used Ziegler−Natta catalytic systems is still missing. Recently, well-defined homogeneous and octahedral complexes that polymerize propene to polypropylenes with microstructures extremely similar to those of polymers produced with the traditional catalysts were discovered. These catalysts offer the exciting opportunity to achieve insights into the mechanism of stereocontrol operative with the traditional catalytic systems.

1. Historical Introduction

"Nature synthesizes many stereoregular polymers, for example, cellulose and rubber. This ability has so far been thought to be a monopoly of Nature operating with biocatalysts known as enzymes. But now Professor Natta has broken this monopoly."[1] These words were used to award the Nobel laureates Karl Ziegler and Giulio Natta in 1963. Ziegler−Natta catalysts are formed in the reactions of transition metal compounds of groups 4−10 (mainly Ti, V, and Zr) with alkyls or hydrides of groups 1, 2, 13, or 14. Many industrially relevant thermoplastic polymeric materials (polyethylene, isotactic polypropylene) and rubbers (polybutadiene, polyisoprene, and ethene−propene copolymers) are produced with Ziegler−Natta catalysts. Ziegler discovered these catalytic systems in 1953, while Natta discovered the synthesis of stereoregular polymers in 1954 by using similar catalytic systems.[1]

Polymers from 1-alkenes are stereoregular if the succession of the configurations of the tertiary C atoms along the main chain is regular.[2] Scheme 1 shows the typical representation of the different types of stereoisomerism present in polymers from 1-alkenes: (i) isotactic sequence of configurations; (ii) syndiotactic sequence of configurations; (iii) no order present, atactic sequence of configurations.

Scheme 1

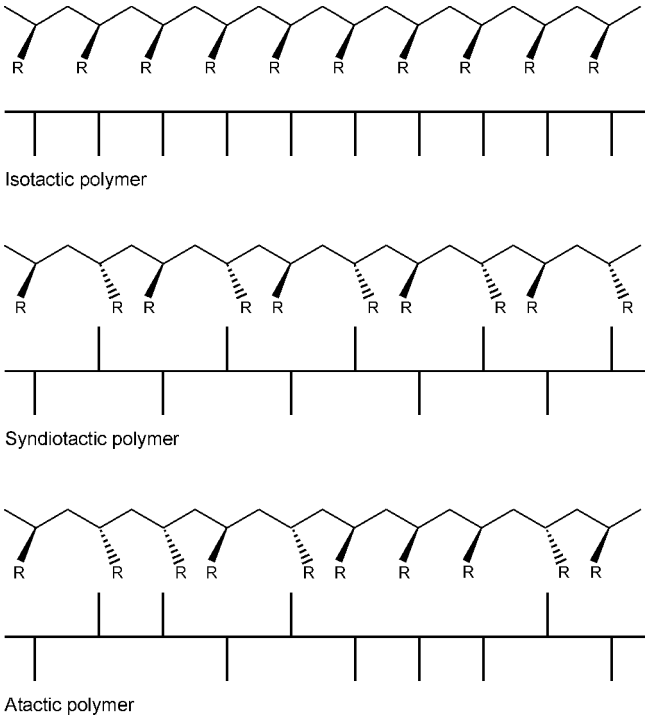

The overall configuration of poly-1-alkenes can be defined using local configurations. Scheme 2 shows that two successive monomeric units (a "diad") can have two nonequivalent relative configurations labeled as meso (or m) and racemic (or r) diads. Therefore, ideally iso- and syndiotactic polymers are characterized by all m and all r diads, respectively.

Scheme 2

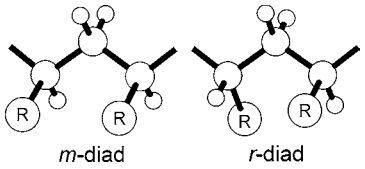

Isotactic poly-1-alkenes are produced with heterogeneous $TiCl_3$ or $TiCl_4/MgCl_2$ catalysts activated by aluminum alkyls, and the amount of m diads in isotactic

Paolo Corradini worked with Giulio Natta in Milano at the discovery of stereoregular polyhydrocarbons. After this exciting experience, he was appointed Full Professor of General and Industrial Chemistry at the University of Napoli. He always shared his interests between the mechanisms of 1-alkene polymerization and the structure of the obtained polymers. He is a permanent member of the Accademia dei Lincei, Rome.

Gaetano Guerra received his Ph.D. in Chemistry working with Corradini. After a short industrial experience, he worked at the University of Napoli for several years. In 1995, he moved to the University of Salerno as Full Professor of Macromolecular Science. His interests are centered on the mechanisms of polymerization of unsaturated hydrocarbons and on the structure of polymeric materials, and he recently became interested in host−guest interactions in polymeric clathrates.

Luigi Cavallo earned his Ph.D. in Chemistry under the supervision of Corradini. After a few years of activity in Napoli, he moved to the University of Salerno in 2002 as Professor of Industrial Chemistry. He likes to understand theoretically the mechanisms of industrially relevant reactions and to develop computational methodologies.

* To whom correspondence should be addressed. E-mail: lcavallo@unisa.it.
† Università di Napoli.
‡ Università di Salerno.

10.1021/ar030165n CCC: $27.50
Published on Web 03/25/2004

Scheme 3

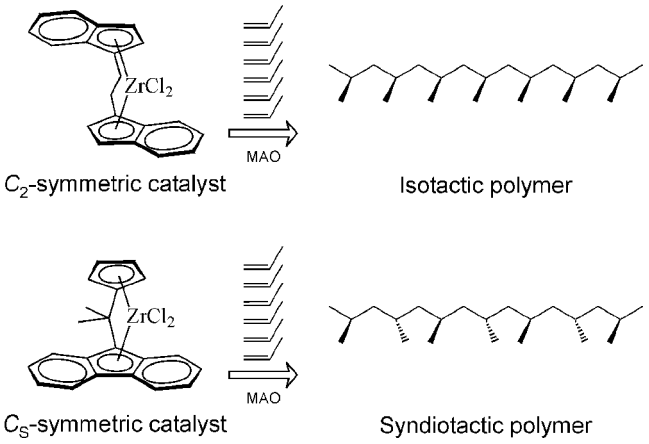

Scheme 4

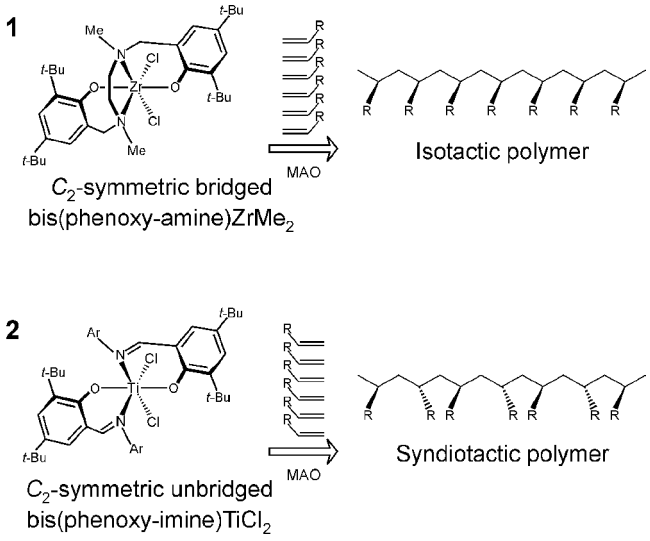

polypropylene can be higher than 99%.[3] Heterogeneous catalysts produce small amounts of syndiotactic poly-1-alkenes, which were instead produced with homogeneous vanadium-based catalysts (VCl_4 or V(III) β-diketonates) activated by aluminum alkyls. The amount of r diads in these syndiotactic polypropylenes can reach 85%.[4] For almost 30 years, the development of these catalysts was substantially limited to technological improvements rather than to a search for new catalysts. The major step forward was achieved around 1970, when titanium chloride species were supported on a matrix, usually crystalline $MgCl_2$.[3]

Attempts to provide homogeneous and chemically more defined (and hence understandable) catalysts immediately followed. However, the early catalysts based on $Cp_2MtCl_2/AlRCl_2$ (Mt = Ti or Zr and Cp = cyclopentadienyl) met with limited success.[5,6] The serendipitous discovery of the activating effect of small amounts of water on the $Cp_2MtX_2/AlMe_3$ system and the subsequent controlled synthesis of methylalumoxane (MAO) by Sinn and Kaminsky in 1976,[7] provided a potent cocatalyst able to activate group 4 metallocenes toward the polymerization of ethene and virtually any 1-alkene. Thanks to the work of Brintzinger, chiral and stereorigid group 4 metallocenes were available, and Ewen used these compounds for the synthesis of stereoregular polymers.[8,9] Depending on the metallocene π-ligand, these systems present completely different stereospecific behaviors. Scheme 3 shows that C_2-symmetric metallocenes polymerize 1-alkenes to isotactic polymers, while C_s-symmetric metallocenes polymerize 1-alkenes to syndiotactic polymers. After many years, the efforts of the scientific community to produce iso- and syndiotactic polymers with well-defined homogeneous catalysts succeded.

The "metallocene revolution" led to an impressive understanding and control of alkene polymerization. Knowledge at the atomic level of many mechanistic details allowed for catalyst tailoring, and the homogeneous catalysts proved to be more flexible than the heterogeneous counterparts. The new catalysts were tuned to (i) obtain several new stereoregular polymers, in particular of a series of new crystalline syndiotactic polymers, (ii) obtain a better control of the molecular mass distribution, (iii) synthesize copolymers with better controlled composition and distribution of the comonomers, and (iv) synthesize low-density polyethylenes with long chain branches.[10−12]

Metallocenes gave the stimulating opportunity to investigate much better defined catalysts, since the coordination of the π-ligands in the catalytic models can be assumed to be similar to those observed in the crystal structures of the precursor metallocenes. Although impressive, the mechanistic understanding of the metallocene catalysts shed light on the traditional catalysts indirectly. In fact, the geometry around the metal atom in metallocenes is pseudotetrahedral, whereas the models proposed for the traditional systems (both for the titanium-based isospecific heterogeneous systems and the vanadium-based syndiospecific homogeneous systems) is usually octahedral.

This situation changed recently with the discovery of well-defined complexes with an octahedral geometry around the metal atom that polymerize 1-alkenes to isotactic polymers (mmmm pentads ∼80%),[13] see Scheme 4, and to syndiotactic polymers (rrrr pentads ∼96%).[14−16] Bridged bis(phenoxy-amine)zirconium-based catalysts produce isotactic polymers,[13] while unbridged bis(phenoxy-imine)titanium-based catalysts produce syndiotactic polymers.[14−16] It is remarkable that both of these catalysts are C_2-symmetric, as the isospecific metallocenes and as the models proposed for the traditional heterogeneous and homogeneous catalysts.

Here, we compare the models developed to explain the origin of stereoselectivity for the well-defined new octahedral systems, and we will revisit the models developed years ago to explain the experimental iso- and syndiospecificity of the traditional Ziegler−Natta catalysts. A close comparison between the new and the traditional catalysts could allow us to understand better the old but industrially used catalysts. The mechanisms presented are based on combined quantum mechanics/molecular mechanics calculations that we performed.

Scheme 5

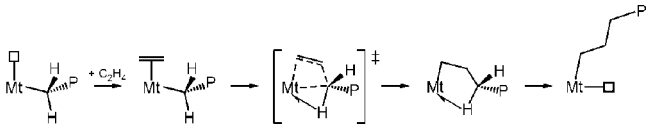

Scheme 6

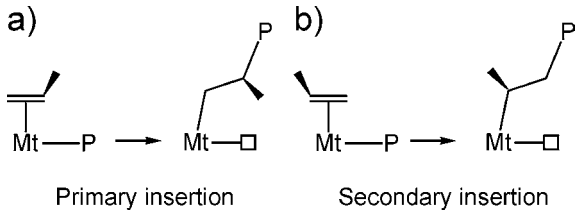

2. Mechanistic Background and Elements of Chirality

The mechanism accepted for chain propagation in the polymerization of 1-alkenes catalyzed by transition metals was proposed by Cossee in 1964.[17] This mechanism is monometallic, and the active center is a transition metal−carbon bond (Scheme 5). It basically occurs in two steps: (i) alkene coordination to a vacant site; (ii) alkene insertion into the metal growing chain bond through a cis opening of the alkene double bond. Green, Rooney, and Brookhart slightly modified this mechanism, introducing an α-agostic interaction, which would facilitate the insertion reaction.[18,19]

Polymerization of 1-alkenes requires we recall the concepts of regio- and stereochemistry of monomer insertion. Regiochemistry of 1-alkenes polymerization can occur via 1,2 (or primary) as well as via 2,1 (or secondary) insertion and lead to growing chains with a primary or a secondary C atom bonded to the metal atom, respectively (Scheme 6). Primary insertion is dominant with the traditional heterogeneous catalysts, with group 4 metallocenes, and with the bridged bis(phenoxy-amine)zirconium-based catalysts, whereas secondary insertion is dominant with the traditional vanadium-based homogeneous catalysts and with the unbridged bis(phenoxy-imine)titanium-based catalysts.

Stereochemistry of monomer insertion is connected to the 1-alkene enantioface that inserts into the Mt growing chain bond. Scheme 7 shows how coordination of the two enantiofaces of a prochiral 1-alkene gives rise to chiral si and re 1-alkene coordinations.[20] Considering the definition of iso- and syndiotactic polymers, isotactic polymers are generated by multiple insertions of 1-alkene molecules with the same enantioface (either re or si), while syndiotactic polymers are generated by a regular alternation of insertions of re and si coordinated monomers.

Stereoselection between the two monomer enantiofaces requires chiral active species, and the elements of chirality usually present in these catalysts are as follows:

(i) The chirality of the active site due to the coordination of the ligands to the metal. In the case of octahedral complexes with two bidentate ligands such as those proposed for the traditional Ziegler−Natta catalysts, as well as for the new century catalysts of Scheme 4, the

Scheme 7

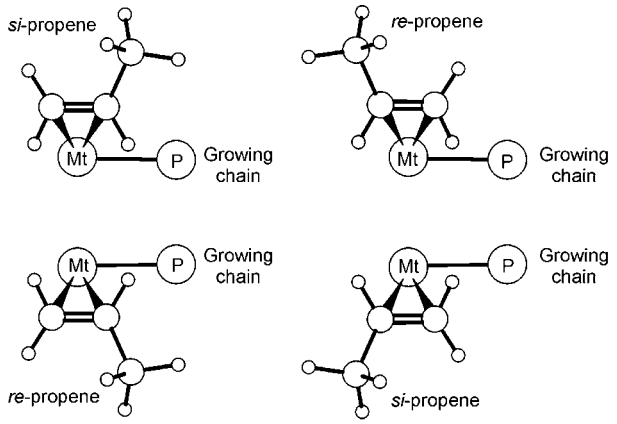

Scheme 8

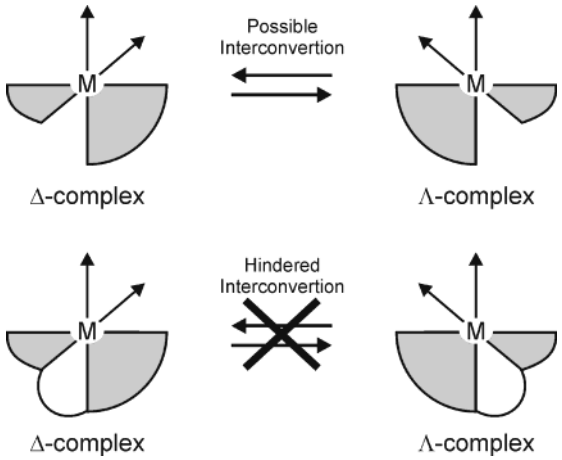

Scheme 9

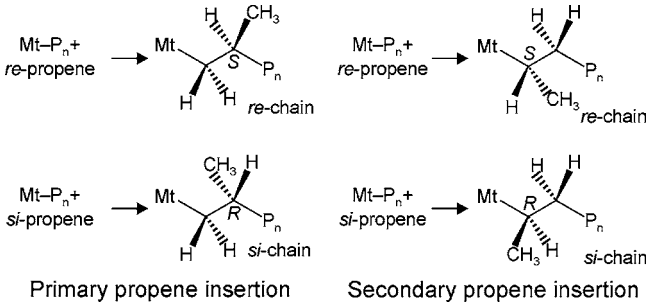

relative orientations of the two bidentate ligands is chiral and can be labeled with the Λ or Δ nomenclature (see Scheme 8).[21−23] If the two bidentate ligands are not bridged, interconversion between different configurations is relatively easy, whereas the presence of chemical bonds that connect the two ligands confers stereorigidity, freezing the configuration at the metal atom (at least in the time scale of a polymerization reaction).

(ii) The chirality of the last tertiary C atom of the growing chain, which is determined by the chirality of monomer coordination in the last insertion step (see Scheme 9). Although the R/S CIP nomenclature could be used,[24] for clarity, we label the two configurations as si- or re-ending growing chains. It is then straightforward that

Scheme 10

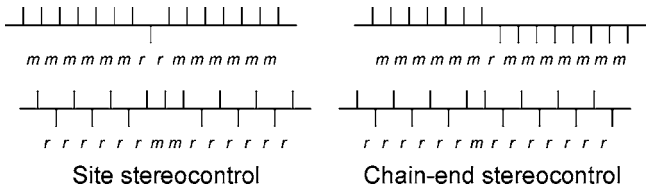

Scheme 11

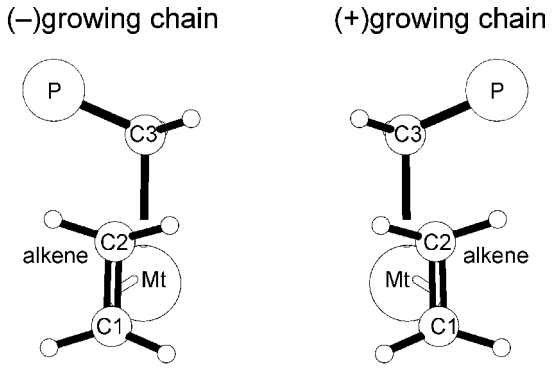

insertion of a re-coordinated monomer on a re-ending or on a si-ending growing chain would lead to an m or to an r diad, respectively. This chirality depends only on the chirality of the last inserted monomer and can change during polymerization if there is a switch in the chirality of monomer insertion.

Both the above elements of chirality can be at the origin of stereoselectivity. If discrimination between the faces of the inserting prochiral monomer is dictated by the chirality of the catalytic site, we are in the presence of *chiral-site stereocontrol*, while we are in the presence of *chain-end stereocontrol* if discrimination is dictated by the chirality of the last inserted monomer unit. The relative amounts of stereodefects in the polymer chain, easily determined with standard NMR techniques,[25,26] indicate which kind of stereocontrol is operative. Bernoullian statistics are consistent with chain-end stereocontrol,[27] while non-Bernoullian distributions originate from chiral-site stereocontrol.[28] The difference can be readily realized for isotactic propagation. Intuitively, for chain-end stereocontrol a stereomistake is propagated, while for chiral-site stereocontrol the same stereomistake, having no effect on the site chirality, remains isolated (see Scheme 10).

Finally, we define a conformational chirality connected to the placement in space of the growing chain. The chiral orientation of the growing chain is determined by the sign of the dihedral angle X_{OI}–Mt–C3–P (X_{OI} is the midpoint of the C1═C2 bond) defined in Scheme 11. Following IUPAC recommendations for stereochemistry,[29] we label the two chiral orientations of the growing chain of Scheme 11 as (−) or (+) growing chains. This chirality is extremely flexible, since it depends only on the conformation assumed by the growing chain before/during formation of the new C–C bond.

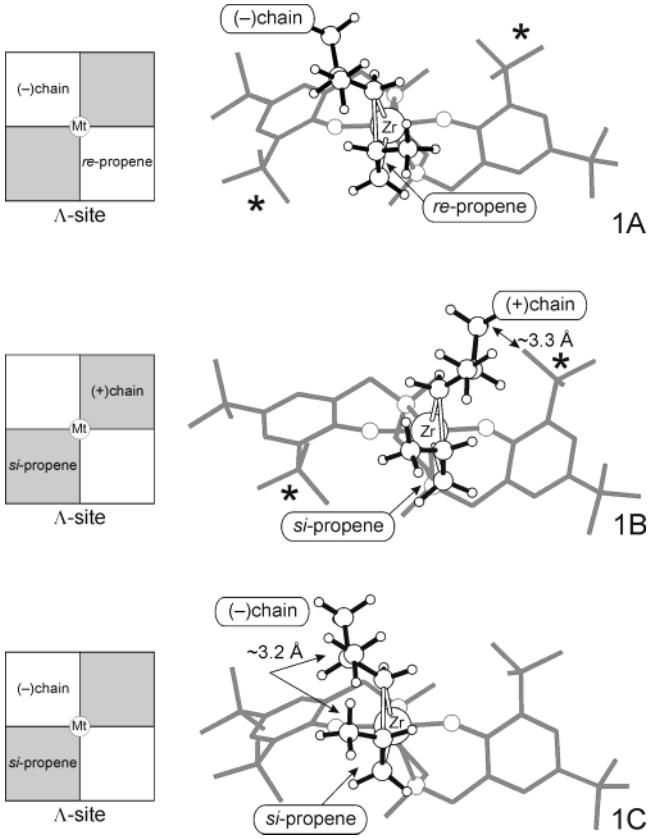

FIGURE 1. Low-energy transition states (right) for propene insertion into a zirconium (primary chain) bond and quadrants representation (left) of the same systems. Gray quadrants correspond to relatively crowded zones occupied by the *t*-Bu groups marked by a star on the right.

3. Chiral-Site Stereocontrol: Isotactic Polypropylene by Primary Propene Insertion

3.1. New Century Bridged Octahedral Catalysts. Low-energy transition states for primary propene insertion into the zirconium–isobutyl bond (which simulates a primary growing chain) are reported in Figure 1 for complex **1** of Scheme 4. In both structures, the configuration of the octahedral active species is Λ, while the enantioface of the inserting propene is re in structure **1A** and si in **1B**. The most stable transition state corresponds to insertion of a *re*-propene on a (−)chain, and it shows the most classical features, which characterize the *mechanism of the chiral orientation of the growing chain*.[21] These are as follows: (i) the growing chain assumes a chiral orientation to minimize steric interactions with the chiral ligand; (ii) the monomer inserts with the methyl group trans oriented relative to the growing chain to minimize its steric interaction with the growing chain itself. Structure **1B** is 1.6 kcal/mol higher in energy relative to structure **1A** because of steric interactions between the (+)chain and the chiral ligand. In this structure, the growing chain is oriented toward one of the *t*-Bu groups, and short distances between the growing chain and the ligand (see Figure 1) indicate steric stress.

These situations are schematically sketched in the quadrants representation of Figure 1. Gray quadrants

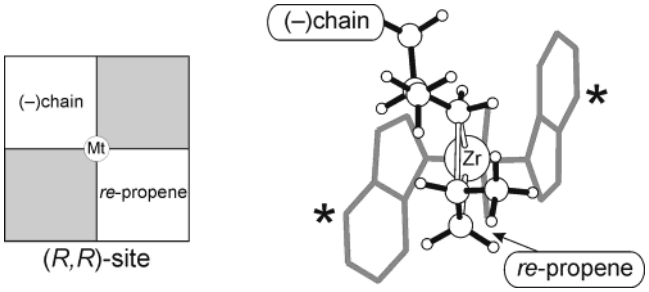

FIGURE 2. Low-energy transition state (right) for propene insertion into a zirconium (primary chain) bond on a typical metallocene catalyst and quadrants representation (left) of the same system. Gray quadrants correspond to relatively crowded zones occupied by the C atoms marked by a star on the right. (*R,R*) is the chirality of coordination of the two indenyl rings.

represent regions sterically occupied by the ligand, while white quadrants are relatively free zones not occupied by the ligand. The lowest-energy transition state places both the chain and the propene methyl group in an open quadrant. This corresponds to a (−)chain/*re*-propene combination of chiralities, whereas the (+)chain/*si*-propene combination is of higher energy since the chain is in a crowded quadrant (steric interactions between the propene and the ligand were calculated to be negligible in **1B**).

This suggestes that the origin of stereoselectivity in site-controlled primary propene polymerization is not due to direct interactions between the monomer and the chiral site. Instead, it is mediated by the chiral orientation of the growing chain, imposed by the site chirality. The chirally oriented growing chain selects between the two enantiofaces of the inserting propene molecule. Since this complex is stereorigid, that is, interconversion between Λ and Δ configurations is frozen (see Scheme 8), at each insertion step the (−)chain/*re*-propene transition state is favored for a Λ-complex. This ensures the formation of an isotactic polymer. Of course, for reasons of symmetry the (+)chain/*si*-propene transition state is favored for a Δ-complex.

The mechanism of the chiral orientation of the growing chain was also used to rationalize the stereospecificity of propene polymerization with group 4 metallocenes (see Scheme 3). The favored transition state for propene insertion on the isospecific catalyst containing the bis(1-indenyl) ligand is shown in Figure 2.[12] The overall similarity with structure **1A** and the same quadrants representation (compare Figures 1 and 2) nicely support a unified view of the mechanisms of stereoselectivity with octahedral and tetrahedral catalysts based on group 4 metals.

3.2. Traditional Titanium-Based Heterogeneous Ziegler−Natta Catalysts. The mechanism of the previous section was first proposed to explain the origin of stereoselectivity in primary propene insertion with the traditional heterogeneous catalysts. Figure 3 reports the most stable transition states for primary propene insertion into the titanium−isobutyl bond of a generic $TiCl_3$ neutral species with a local C_2 symmetry. In these structures, the configuration of the octahedral active species is Δ, while

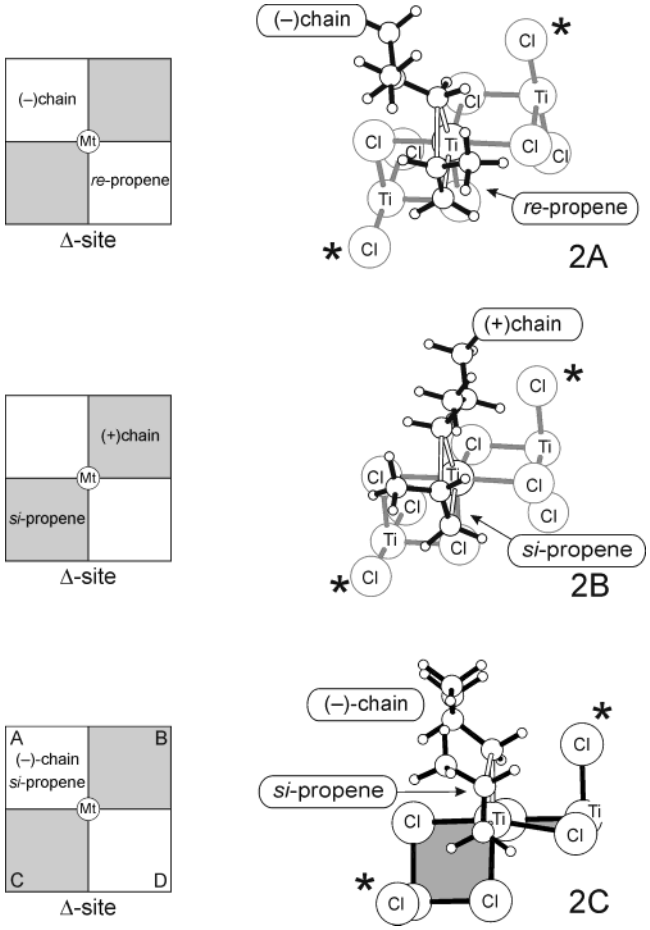

FIGURE 3. Low-energy transition states (right) for propene insertion into a titanium (primary chain) bond and quadrants representation (left) of the same systems. Gray quadrants correspond to crowded zones occupied by the Cl atoms marked by a star on the right.

the enantioface of the inserting propene is re in **2A** and si in **2B**. The most stable structure **2A** corresponds to the (−)chain/*re*-propene combination of chiralities. The relative geometry of the growing chain and of the monomer in **2A** and **1A** is strongly similar. Structure **2A** is favored relative to **2B** by 2.7 kcal/mol because in the latter the growing chain interacts repulsively with the nearby halide atom marked with a star. Moreover, the growing chain is tightened (tethered) in its movements by the nearby ligands much more in **2B** than in **2A**. This may give rise to unfavorable entropic contributions that could increase the total free energy difference in favor of **2A**.

The quadrants representation indicates that space occupation or, equivalently, the shape of the chiral pocket casted by the ligands of the systems of Figures 1 and 3 is the same because the main sources of steric stress, the *t*-Bu groups and the Cl atoms, occupy relatively similar zones. Remarkably, this occurs despite of the opposite configuration of the octahedral complexes (Λ in Figure 1 and Δ in Figure 3). Since space occupation is relevant, and not the absolute configuration of the active species, the same (−)chain/*re*-propene combination of chiralities is favored in both cases since it minimizes steric interactions at the transition state.

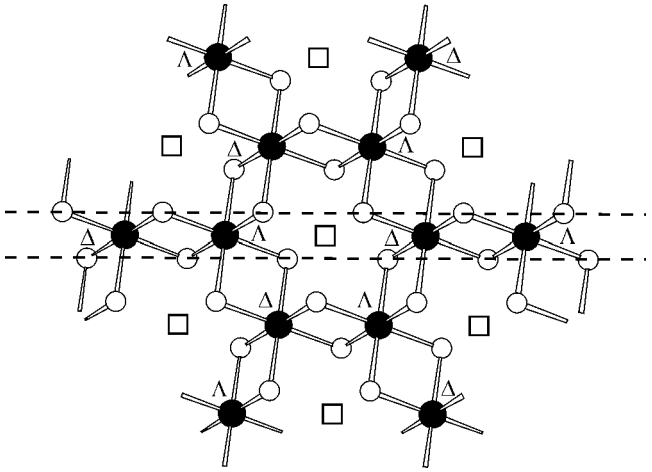

FIGURE 4. Structural layer of violet $TiCl_3$. Ti atoms (full circles) are bonded to six Cl atoms (empty circles); vacant octahedral positions are indicated by squares. Dashed lines correspond to the lateral cut of Figure 5.

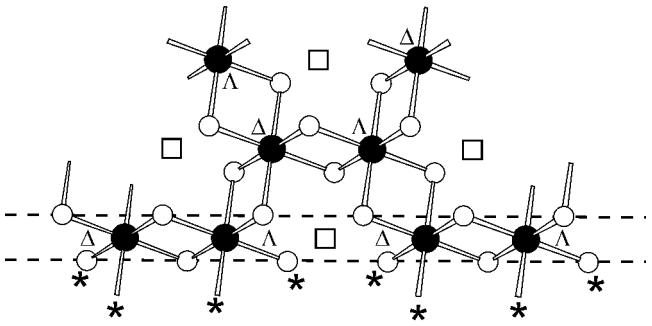

FIGURE 5. Possible lateral cut of a $TiCl_3$ layer. Nonequivalent coordination positions, which will become available to monomer and growing polymer chain, are indicated by a star.

After we showed that this mechanism explains the origin of stereoselectivity in a well-defined homogeneous catalyst and in a hypothetical model of the heterogeneous Ziegler−Natta catalysts, we discuss the formation of possible active Ti species on the traditional $TiCl_3$ and $MgCl_2/TiCl_4$ catalytic systems. The characterization of heterogeneous Ziegler−Natta catalysts at atomic level is still matter of research.

Natta hypothesized that steric control is due to the structure of catalytic sites on the border of crystal layers of $TiCl_3$,[30] and Arlman and Cossee developed this idea in detail.[31] Violet $TiCl_3$ and other transition metal trichlorides effective as Ziegler Natta catalysts (e.g., VCl_3, $CrCl_3$), are built by layers as that of Figure 4, stacked one on top of the other according to a close packing of the chlorine atoms. Within each layer, the metal atoms neatly occupy two-thirds of the octahedral positions, and neighboring metal atoms (bridged by two Cl atoms) have opposite configurations, which may be labeled as Λ and Δ.[21,22]

Figure 5 illustrates that, if we cut a $TiCl_3$ layer parallel to the line connecting two bridged Ti atoms, electroneutrality conditions impose that each Ti atom at the surface is bonded to five Cl atoms only. Four of these Cl atoms are more strongly bonded to the Ti atoms because they

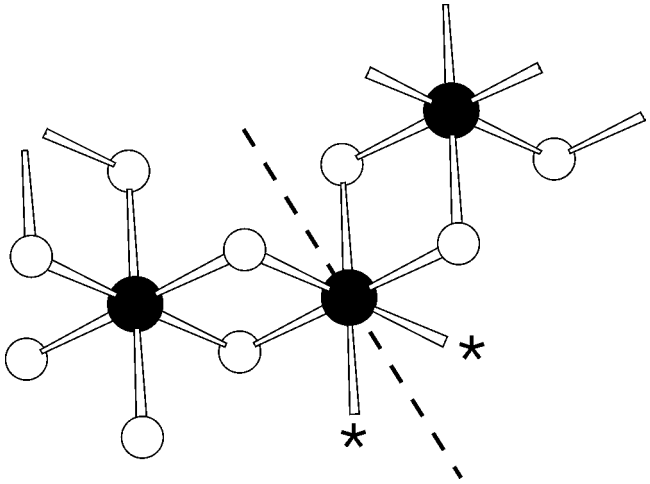

FIGURE 6. A different lateral cut of a $TiCl_3$ layer. The dashed line indicates the local 2-fold axis.

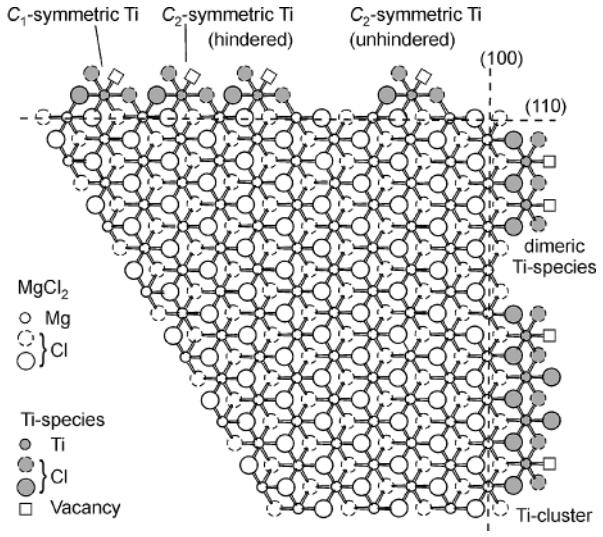

FIGURE 7. Structural layer of $MgCl_2$. Full line Cl atoms represent Cl atoms above the plane of the Mg atoms, whereas dashed Cl atoms represent Cl atoms below the plane of the Mg atoms. Possible (100) and (110) lateral cuts with 5- and 4-coordinated Mg atoms are indicated. Possible Ti^{III}-chloride species with different steric environments are represented.

are bridged to further metal atoms. The fifth Cl atom, nonbridged, may be replaced by an alkyl group. The free sixth octahedral position may coordinate an alkene. For these sites, the two positions accessible to the growing chain and to the monomer are nonequivalent. Thus, these hypothetical catalytic sites would be C_1 symmetric.

Active sites with Ti atoms bonded to four Cl atoms only (Figure 6) were proposed by Allegra.[32] The octahedral coordination positions available to the monomer and the growing chain (indicated by stars in Figure 6) are equivalent because the surface atoms with relevant nonbonded interactions at the catalytic site present a local C_2 symmetry. Thus, this site would behave as the octahedral catalyst of section 3.1.

As for $MgCl_2$-supported catalysts, $MgCl_2$ has crystal structures somewhat similar to those of violet $TiCl_3$. This dictates the possibility of an epitaxial coordination of $TiCl_4$

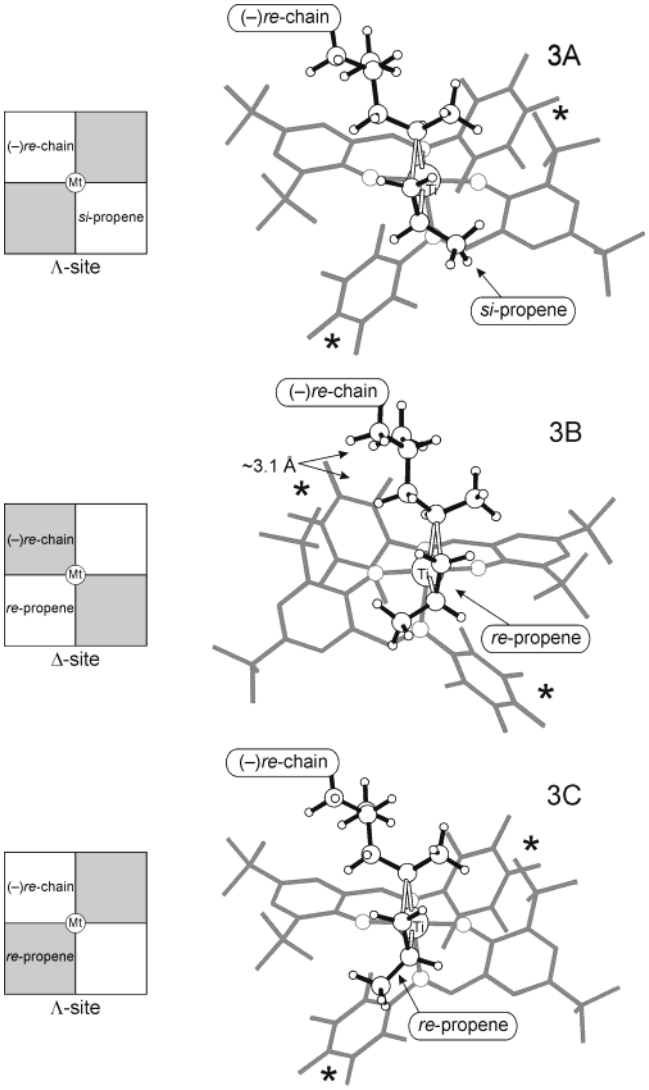

FIGURE 8. Transition states (right) for propene insertion into a titanium (secondary chain) bond and quadrants representation (left) of the same systems. Gray quadrants correspond to relatively crowded zones occupied by the *t*-Bu groups marked by a star on the right.

units (or $TiCl_3$ units after reduction) on the lateral faces of $MgCl_2$ crystals.[33]

The epitactic placement of Ti_2Cl_6 and Ti_4Cl_{12} units on the (100) face of $MgCl_2$ is shown in Figure 7. The environment of the Ti atoms is chiral and the dimeric Ti^{III} sites on the (100) cut are very similar to the C_1 symmetric sites proposed by Cossee,[31] while the terminal Ti atoms of polynuclear Ti^{III} sites (with $n > 2$)[34] are extremely similar to the C_2 symmetric sites proposed by Allegra for $TiCl_3$-based catalytic systems.[32]

On the (110) face there are many possibilities. Although an isolated titanium species adsorbed on the (110) face can be thought to produce a poorly stereoregular polymer with a prevalence of syndiotactic diads,[34] C_1- and C_2-symmetric titanium species, which could produce isotactoid and isotactic polymers, are obtainable by occupation of one and two vicinal positions. The species that could originate steric bulkiness close to the active titanium atom could be other titanium chloride species, as shown in Figure 7, or aluminum species and the Lewis bases. A possible role of these bases could be an enforced packing of the different species on the lateral cuts, thus increasing the number of active titanium species with a sterically congested environment.

4. Chain-End Stereocontrol: Syndiotactic Polypropylene by Secondary Propene Insertion

4.1. New Century Unbridged Octahedral Catalysts. Low-energy transition states for secondary propene insertion into the titanium (growing chain) bond (the secondary growing chain is simulated by the chiral $-CH(CH_3)CH_2-CH(CH_3)_2$ group) are reported in Figure 8 for complex **2** of Scheme 4. All the structures present a re-ending chain, which is a chain originated from secondary insertion of a re-coordinated propene. The configuration of the chiral complexes is Λ in **3A** and **3C**, while it is Δ in **3B**. The enantioface of the inserting propene is si in **3A** and re in **3B** and **3C**. Finally, the secondary re-growing chain is forced to assume always a (−) orientation to form a stabilizing α-agostic interaction.

Structure **3A** is more stable than **3B** and **3C** by 1.4 and 3.6 kcal/mol, respectively. Structure **3A** corresponds to insertion of a *si*-propene on a complex with a (−)*re*-chain/Λ-site configuration. In this structure, the chiral growing chain is oriented far away from the bulky substituents of the ligand, while the monomer inserts with the enantioface that minimizes steric interactions with the ligand.[35] Structure **3C**, with the same (−)*re*-chain/Λ-site configuration of **3A** but a different propene enantioface, is disfavored by steric interactions between the methyl group of the inserting *re*-propene with the ligand skeleton.

The quadrants representation of Figure 8 illustrates that **3A** is favored because both the growing chain and the methyl group of the inserting propene are placed in uncrowded quadrants. This implies that a Λ-site is favored over a Δ-site, since in the latter the growing chain would lay in a sterically congestioned quadrant (structure **3B**). Since a Λ-site is favored by the *re*-chain (due to its (−) orientation), insertion of a *re*-propene is disfavored because the propene methyl group would be placed in a congestioned quadrant (structure **3C**).

Scheme 12 illustrates the sequence of events that may occur during polymerization. Insertion of a si-coordinated propene on a (−)*re*-chain/Λ-site active species generates a *si*-chain/Λ-site active species. An active species with this configuration is disfavored by steric interaction of the growing chain with the ligand (to form a α-agostic hydrogen bond the *si*-chain must lay in the top-right quadrant, i.e., it must assume a (+) orientation). Instead, site isomerization to a Δ-site active species would easily accommodate a *si*-chain and its (+) orientation. The (+)-*si*-chain/Δ-site active species then leads to a relatively low-energy path for insertion of a re-coordinated propene through a transition state that is the mirror image of **3A** (compare left and right sides of Scheme 12). In agreement with the experiments, this implies a syndiospecific enchainment.

Scheme 12

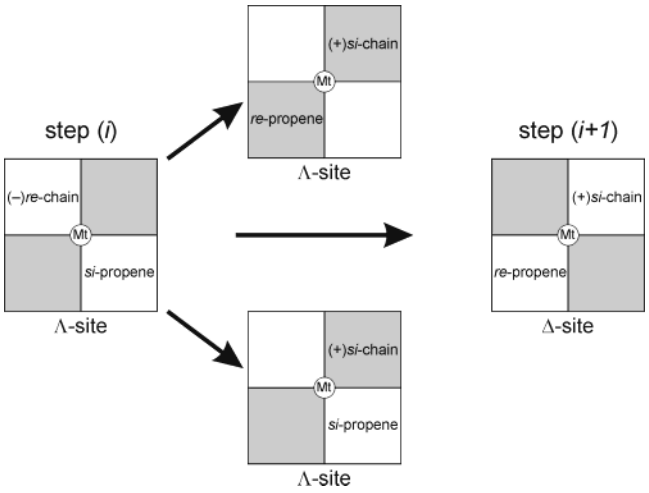

Scheme 13

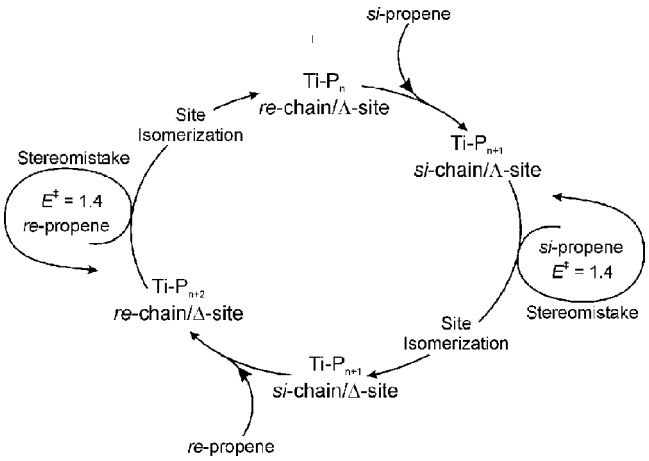

Scheme 14

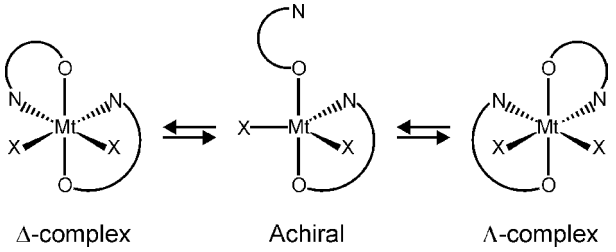

The above considerations lead to the possible polymerization cycle of Scheme 13. Of course, the ability of the active site to adjust its configuration to that of the growing chain at each insertion step is a mandatory requirement.

Existence of these fluxional equilibria in related neutral complexes was proved with NMR experiments, which resulted in barriers for the interconversion close to 15 kcal/mol.[36,37] Site isomerization was proposed to occur with the dissociative mechanism of Scheme 14. We calculated the binding energy of the N-imine atoms (which should be a good approximation to the energy barrier of the site-isomerization process) in the cationic monomer-free and monomer-bound species, which could be the resting state and the intermediate that precedes insertion, respectively. The N binding energy in the

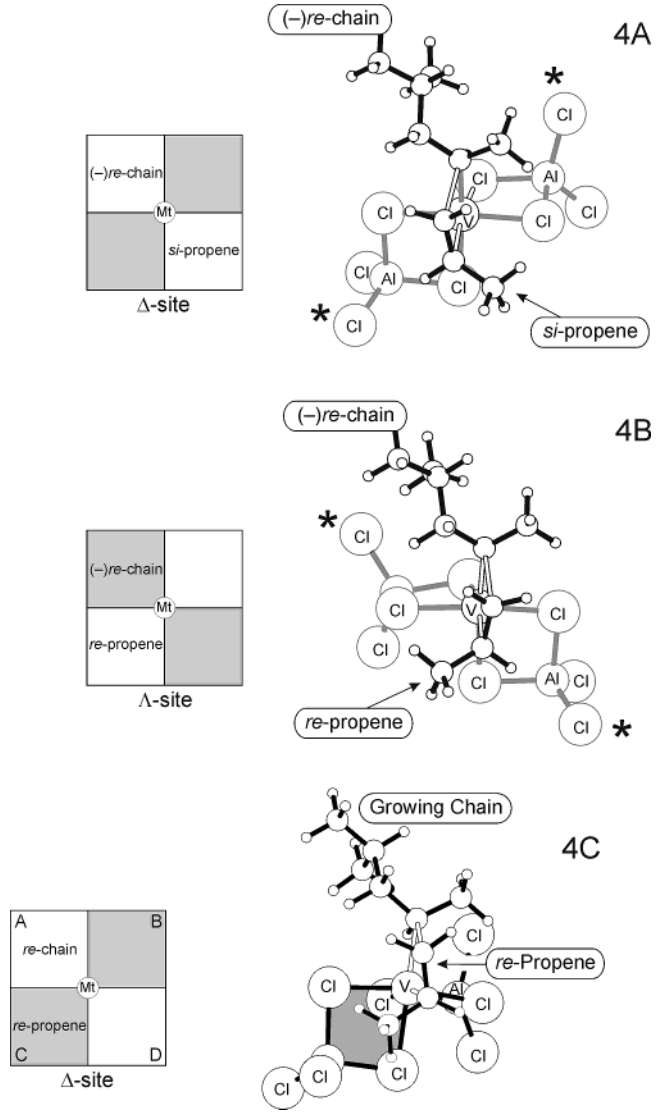

FIGURE 9. Low-energy transition states for propene insertion into a vanadium (secondary chain) bond and quadrants representation (left) of the same systems. Gray quadrants correspond to crowded zones occupied by the Cl atoms marked by a star on the right.

monomer-free species is close to 25 kcal/mol, while in the monomer-bound species it is sligthly lower than 15 kcal/mol. Barriers of this height could be comparable with the overall barrier of propene insertion, considering the relatively slow propagation rate and scarce activity of these catalysts.

4.2. Traditional Vanadium-Based Homogeneous Ziegler−Natta Catalysts. The mechanism of the previous section was first proposed[22] to explain the origin of stereoselectivity in secondary and syndiospecific chain-end controlled polymerization of propene with the homogeneous vanadium-based catalytic systems,[38] still used for the industrial production of ethene−propene copolymers. Also in that case the origin of syndiospecificity was supposed to be based on the formation of a fluxional chiral site. The assumed model consisted of a hexacoordinated vanadium atom surrounded by four chlorine atoms assumed to be bridge-bonded to other metal atoms (the aluminum atoms of the AlR_3 cocatalysts, for ex-

ample).[4,22,39] Thus, the catalytic site is chiral and, similar to the homogeneous bis(phenoxy-imine)titanium catalyst of the previous section, interconversion between enantiomeric complexes is assumed to be possible.[22]

In Figure 9, we report the most stable transition states for secondary propene insertion into the vanadium (growing chain) bond (the secondary growing chain is simulated by the chiral $-CH(CH_3)CH_2CH(CH_3)_2$ group). Both structures present a re-ending chain. The configuration of the chiral complexes is Δ in **4A**, while it is Λ in **4B**. The enantioface of the inserting propene is si in **4A**, and re in **4B**.

Structure **4A** is more stable than **4B** by 1.2 kcal/mol. Thus, the favored transition state corresponds to insertion of a si-coordinated propene on a complex with a (−)*re*-chain/Δ-site configuration, and it is rather similar to **3A** of Figure 8. In both structures, the chiral growing chain (the chirality of which is fixed by the enantioface of the last inserted propene molecule) favors a site configuration (which is fluxional) that minimizes steric interactions between the growing chain and the ligand skeleton. The favored (−)*re*-chain/Δ-site of the vanadium-based catalysts and the (−)*re*-chain/Λ-site of the bis(phenoxy-imine)titanium catalysts, constitute a chiral pocket that inserts easily a *si*-propene, structures **4A** and **3A**, thus generating an r diad. Formation of an m diad, structures **4B** and **3B**, is disfavored by steric interactions of the chiral growing chain with the ligand skeleton.

The quadrants representation indicates that the shape of the chiral pocket casted by the ligands of the systems of Figures 8 and 9 is the same because the main sources of steric stress, the *t*-Bu groups and the Cl atoms marked by a star, occupy relatively similar zones. As for the isospecific systems of the previous sections, this occurs despite of the opposite configuration of the octahedral complexes (Λ in **3A** and Δ in **4A**). Since space occupation is relevant and not the absolute configuration of the active species, the same combination of chiralities, (−)*re*-chain/*si*-propene, is favored in both cases since this combination minimizes steric interactions at the transition state.

5. Conclusions

In this Account, we discussed the origin of stereoselectivity in well-defined new century catalysts with an octahedral geometry around the active metal atom, and we tried to use these models to validate similar models that we proposed years ago for the traditional and industrially used Ziegler−Natta catalysts. The models for the latter class were only hypothetical due to the limited experimental characterization of the active species. In particular, we compared the following:

(i) Models for the chiral-site-controlled isospecific primary polymerization of propene by the newly discovered bridged bis(phenoxy-amine)zirconium-based systems with the old heterogeneous $TiCl_3$- and $MgCl_2/TiCl_4$-based systems. In both cases, the geometry around the metal atom is chiral, and the presence of the C−C bridge in the case of the new catalysts and of the crystal matrix

Scheme 15

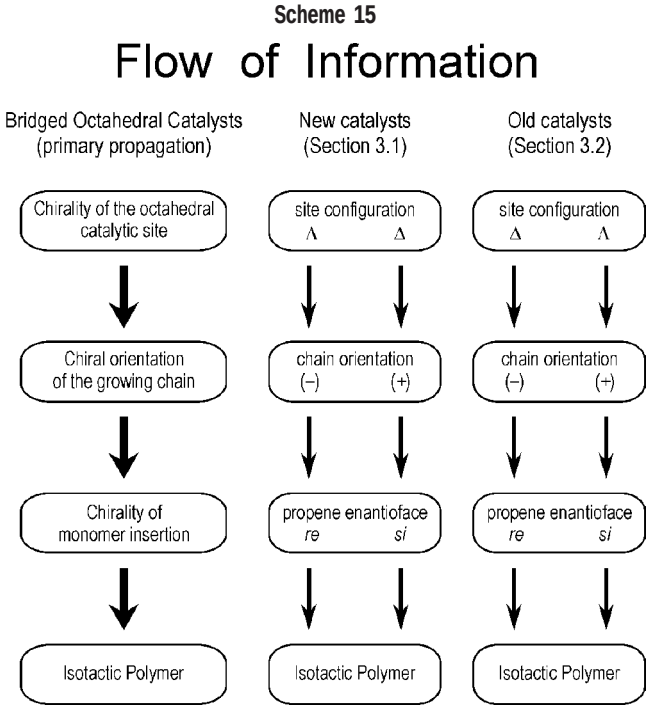

in the case of the old catalytic systems confers stereorigidity to the active species. The origin of stereoselectivity is connected to the chiral orientation of the growing chain, dictated by the chirality of the active site. Selection between the two monomer enantiofaces originates from steric interactions between the chirally oriented growing chain and the propene methyl group.

(ii) Models for the chain-end controlled syndiospecific secondary polymerization of propene by the newly discovered unbridged bis(phenoxy-imine)titanium-based systems with the old homogeneous vanadium-based systems. In both cases, the geometry around the metal atom is chiral, but the absence of a bridge allows for a rapid (compared to the rate of propene insertion) fluxional equilibrium between opposite configurations. The origin of stereoselectivity is connected to the chirality of the last C atom of the growing chain, which dictates the configuration of the active site. Selection between the two monomer enantiofaces originates from steric interactions between the chiral skeleton of the active site and the propene methyl group.

The two mechanisms have some similarities, since in both cases the "crucial" element of chirality at the origin of the enantioselectivity (site chirality for the isospecific and stereorigid systems and chain-end chirality for the syndiospecific and unbridged systems) does not select the enantioface of the inserting monomer directly. In both cases, there is a messenger of information from the "crucial" element of chirality to the monomer. However, the flow of information that originates stereoselectivity is rather different. In fact, Scheme 15 shows that for primary propene insertion with the stereorigid catalysts the chirally oriented growing chain acts as messenger of information between the chiral active site and the inserting prochiral monomer.

Scheme 16

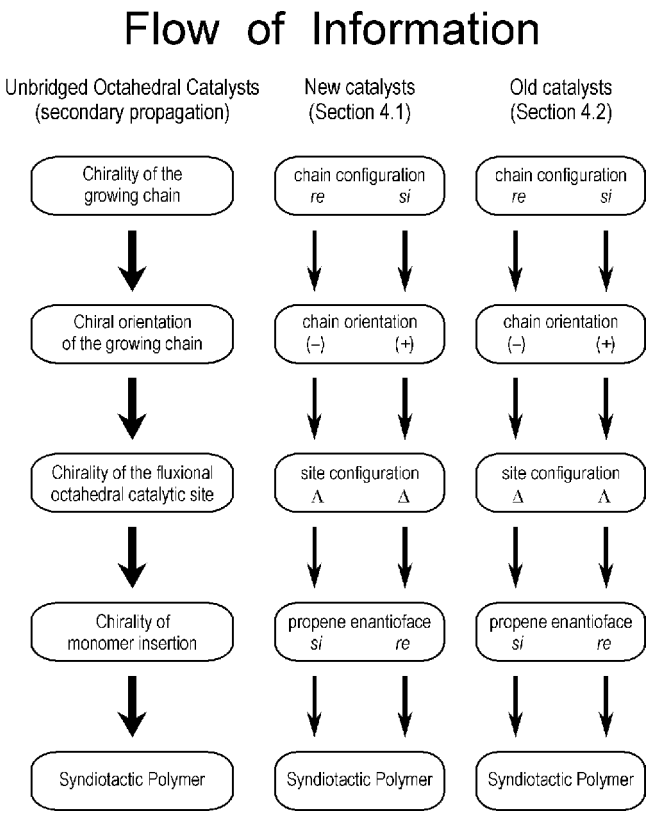

Instead, in the case of secondary propene insertion with the stereoflexible catalysts, Scheme 16 shows that the chirally oriented growing chain acts as a messenger between the chiral growing chain end and the configuration at the metal atom. The so determined chirality of the catalytic site selects between the two enantiofaces of the prochiral monomer.

The financial support of MURST of Italy (Grants PRIN-2002 and FISR) and Basell Polyolefins is gratefully acknowledged.

References

(1) Nobel e-Museum. http://www.nobel.se/chemistry/laureates/1963 (accessed 3/20/2004).
(2) IUPAC − Stereochemical definitions and notations relating to polymers. *Pure Appl. Chem.* **1979**, *51*, 1101−1121.
(3) Moore, E. P. J. *Polypropylene handbook: polymerization, characterization, properties, applications*; Hanser Publishers: Munich, Germany, 1996.
(4) Zambelli, A.; Sessa, I.; Grisi, F.; Fusco, R.; Accomazzi, P. Syndiotactic polymerization of propylene: single-site vanadium catalysts in comparison with zirconium and nickel. *Macromol. Rapid Commun.* **2001**, *22*, 297−310.
(5) Natta, G.; Mazzanti, G. Organometallic complexes as catalysts in ionic polymerizations. *Tetrahedron* **1960**, *8*, 86−100.
(6) Long, W. P.; Breslow, D. S. Polymerization of ethylene with bis-(cyclopentadienyl)titanium dichloride and diethylaluminum chloride. *J. Am. Chem. Soc.* **1960**, *82*, 1953−1957.
(7) Andresen, A.; Cordes, H. G.; Herwig, J.; Kaminsky, W.; Merck, A.; Mottweiler, R.; Pein, J.; Sinn, H.; Vollmer, H. J. Halogen-free soluble Ziegler catalysts for the polymerization of ethylene. Control of molecular weight by choice of temperature. *Angew. Chem., Int. Ed. Engl.* **1976**, *15*, 630−632.
(8) Ewen, J. A. Mechanisms of stereochemical control in propylene polymerizations with soluble Group 4B metallocene/methylalumoxane catalysts. *J. Am. Chem. Soc.* **1984**, *106*, 6355−6364.
(9) Ewen, J. A.; Jones, R. L.; Razavi, A.; Ferrara, J. D. Syndiospecific propylene polymerizations with Group IVB metallocenes. *J. Am. Chem. Soc.* **1988**, *110*, 6255−6256.
(10) Brintzinger, H. H.; Fischer, D.; Mülhaupt, R.; Rieger, B.; Waymouth, R. M. Syndiospecific propylene polymerizations with Group IVB metallocenes. *Angew. Chem., Int. Ed. Engl.* **1995**, *34*, 1143−1170.
(11) Gladyzs, J. A., Ed. Frontiers in Metal-Catalyzed Polymerization. Special issue of *Chem. Rev.* **2000**, *100*, 1167−1682.
(12) Corradini, L.; Guerra, G.; Cavallo, L. Chirality of catalysts for stereospecific polymerizations. *Top. Stereochem.* **2003**, *24*, 1−46.
(13) Tshuva, E. Y.; Goldberg, I.; Kol, M. Isospecific Living Polymerization of 1-Hexene by a Readily Available Nonmetallocene C_2-Symmetrical Zirconium Catalyst. *J. Am. Chem. Soc.* **2000**, *122*, 10706−10707.
(14) Tian, J.; Coates, G. W. Development of a Diversity-Based Approach for the Discovery of Stereoselective Polymerization Catalysts: Identification of a Catalyst for the Synthesis of Syndiotactic Polypropylene. *Angew. Chem., Int. Ed.* **2000**, *39*, 3626−3629.
(15) Saito, J.; Mitani, M.; Onda, M.; Mohri, J.; Ishii, S.; Yoshida, Y.; Nakano, T.; Tanaka, H.; Matsugi, T.; Kojoh, S. I.; Kashiwa, N.; Fujita, T. Microstructure of Highly Syndiotactic "Living" Poly(propylene)s Produced from a Titanium Complex with Chelating Fluorine-Containing Phenoxyimine Ligands (an FI Catalyst). *Macromol. Rapid Commun.* **2001**, *22*, 1072−1075.
(16) Mitani, M.; Furuyama, R.; Mohri, J.-i.; Saito, J.; Ishii, S.; Terao, H.; Kashiwa, N.; Fujita, T. Fluorine- and Trimethylsilyl-Containing Phenoxy-Imine Ti Complex for Highly Syndiotactic Living Polypropylenes with Extremely High Melting Temperatures. *J. Am. Chem. Soc.* **2003**, *124*, 7888−7889.
(17) Cossee, P. Ziegler−Natta catalysis. I. Mechanism of polymerization of α-olefins with Ziegler−Natta catalysts. *J. Catal.* **1964**, *3*, 80−88.
(18) Brookhart, M.; Green, M. L. H.; Wong, L. L. Carbon-hydrogen-transition metal bonds. *Prog. Inorg. Chem.* **1988**, *36*, 1−124
(19) Grubbs, R. H.; Coates, G. W. α-Agostic Interaction and Olefin Insertion in Metallocene Polymerization Catalysts. *Acc. Chem. Res.* **1996**, *29*, 85−93.
(20) Hanson, K. R. Applications of the sequence rule. I. Naming the paired ligands g,g at a tetrahedral atom Xggij. II. Naming the two faces of a trigonal atom Yghi. *J. Am. Chem. Soc.* **1966**, *88*, 2731−2742.
(21) Corradini, P.; Barone, V.; Fusco, R.; Guerra, G. Analysis of models for the Ziegler−Natta stereospecific polymerization on the basis of nonbonded interactions at the catalytic site. I. The Cossee model. *Eur. Polym. J.* **1979**, *15*, 1133−1141.
(22) Guerra, G.; Corradini, P.; Pucciariello, R. New model of the origin of the stereospecificity in the synthesis of syndiotactic polypropylene. *Macromolecules* **1985**, *18*, 2030−2034.
(23) *IUPAC − Nomenclature of Inorganic Chemistry*, 2nd ed. Butterworths: London, 1971. (IUPAC Definitive Rules 1970).
(24) Cahn, R. S.; Ingold, C.; Prelog, V. Specification of molecular chirality. *Angew. Chem., Int. Ed. Engl.* **1966**, *5*, 385−415.
(25) Classical Review: Zambelli, A.; Ammendola, P. Stereospecific polymerization of α-olefins: end groups, polymer structure and reaction mechanism. *Prog. Polym. Sci.* **1991**, *16*, 203−218.
(26) Recent Review: Busico, V.; Cipullo, R. Microstructure of polypropylene. *Prog. Polym. Sci.* **2001**, *26*, 443−533.
(27) Bovey, F. A.; Tiers, G. V. D. Polymer nuclear spin resonance spectroscopy. II. The high-resolution spectra of methyl methacrylate polymers prepared with free radical and anionic initiators. *J. Polym. Sci.* **1960**, *44*, 173−182.
(28) Sheldon, R. A.; Fueno, T.; Tsunetsugu, T.; Furukawa, J. One-parameter model for isotactic polymerization based on enantiomorphic catalyst sites. *J. Polym. Sci., Part B* **1965**, *3*, 23−26.
(29) Moss, G. P. Basic terminology of stereochemistry. *Pure Appl. Chem.* **1996**, *68*, 2193−2222.
(30) Natta, G. Stereospecific polymerization by means of coordinated anionic catalysis. *J. Inorg. Nucl. Chem.* **1958**, *8*, 589−611.
(31) Arlman, E. J.; Cossee, P. Ziegler−Natta catalysis. III. Stereospecific polymerization of propene with the catalyst system TiCl3−AlEt3. *J. Catal.* **1964**, *3*, 99−104.
(32) Allegra, G. Mechanism of polymerization of α-olefins with Ziegler−Natta catalysts. *Makromol. Chem.* **1971**, *145*, 235−246.
(33) Corradini, P.; Barone, V.; Fusco, R.; Guerra, G. A possible model of catalytic sites for the stereospecific polymerization of α-olefins on first-generation and supported Ziegler−Natta catalysts. *Gazz. Chim. Ital.* **1983**, *113*, 601−607.
(34) Monaco, G.; Toto, M.; Guerra, G.; Corradini, P.; Cavallo, L. Geometry and Stability of Titanium Chloride Species Adsorbed on the (100) and (110) Cuts of the $MgCl_2$ Support of the Heterogeneous Ziegler−Natta Catalysts. *Macromolecules* **2000**, *33*, 8953−8962.
(35) Milano, G.; Cavallo, L.; Guerra, G. Site Chirality as a Messenger in Chain-End Stereocontrolled Propene Polymerization. *J. Am. Chem. Soc.* **2002**, *124*, 13368−13369.

(36) Harrod, J. F.; Taylor, K. Intramolecular rearrangements in bis-(chelate)titanium(IV) complexes. *J. Chem. Soc., Chem. Commun.* **1971**, 696−697.
(37) Bei, X.; Swenson, D. C.; Jordan, R. F. Synthesis, Structures, Bonding, and Ethylene Reactivity of Group 4 Metal Alkyl Complexes Incorporating 8-Quinolinolato Ligands. *Organometallics* **1997**, *16*, 3282−3302.
(38) Natta, G.; Pasquon, I.; Zambelli, A. Stereospecific catalysts for the head-to-tail polymerization of propylene to a crystalline syndiotactic polymer. *J. Am. Chem. Soc.* **1962**, *84*, 1488−1490.
(39) Zambelli, A.; Pasquon, I.; Signorini, R.; Natta, G. Polymerization of propylene to syndiotactic polymer. III. Behavior of the catalyst system vanadium tetrachloride-diethylaluminum chloride in the presence of Lewis bases. *Makromol. Chem.* **1968**, *112*, 160−182.

AR030165N